WHIOCE PUBLISHING PTE. LTD.
PROVIDING FIRST-CLASS SCIENTIFIC INFORMATION FOR TOP SCHOLARS

2026 Volume 7, Issue 2
Cell Biology Research
ISSN:2529-7627

Fabrication and Characterization of Poly-(L-Lysine-co-L-Lactide-co-ε-Caprolactone)/Poly-L-Lactic Acid Porous Scaffolds

Gen Zhang[1], Jianjun Fang[1]*, Wenjuan Liu[2], Xiaozhou Cui[1], Sha Liu[1], Yi Lan[4], Chao Zhang[1], Zhihua Zhou[1,2,3]*

[1]School of Chemistry and Chemical Engineering, Hunan University of Science and Technology, Xiangtan 411100, Hunan, China

[2]Hunan Provincial Key Laboratory of Controllable Preparation and Functional Application of Fine Polymers, Hunan University of Science and Technology, Xiangtan 411100, Hunan, China

[3]Hunan Province College Key Laboratory of Molecular Design and Green Chemistry, Hunan University of Science and Technology, Xiangtan 411100, Hunan, China

[4]Guangdong Gaoshun Environmental Technology Co., Ltd., Hunan Branch, Xiangtan 411100, Hunan, China

Author to whom correspondence should be addressed.

Abstract: Three-dimensional porous scaffold materials have been increasingly applied in the field of bone tissue engineering to provide a suitable microenvironment for the propagation of cells. Poly-(L-lysine-co-L-lactide-co-ε-caprolactone)/poly-L-lactic acid (PLL-b-PLA-b-PCL/PLA) porous scaffolds were prepared by using a thermally induced phase separation (TIPS) method. The influences of fabrication parameters, including mass ratio, polymer concentration and freezing temperature, on the morphology, porosity and compressive strength were studied. The optimum conditions for fabrication of the PLL-b-PLA-b-PCL/PLA porous scaffolds were determined as -30 °C, PLL-b-PLA-b-PCL/PLA concentration of 16.0 wt%, and a mass ratio of 1:5 (PLL-b-PLA-b-PCL to PLA) for cell growth and proliferation. The PLL-b-PLA-b-PCL/PLA showed an interconnected porous structure and the pore size was about 30-70 μm. Such PLL-b-PLA-b-PCL/PLA porous scaffolds may be considered as a promising candidate for tissue engineering scaffolds supporting attachment and proliferation of cells.

Keywords: Poly-(L-lysine-co-L-lactide-co-ε-caprolactone); Poly-L-lactic acid; Scaffold; Morphology

Online publication: June 26, 2026

1. Introduction

Bone tissue engineering is an advanced approach to developing functional scaffold materials for repairing and regenerating fractured bone. These functional scaffold materials should be biodegradable and biocompatible, encouraging cell adherence, proliferation and migration to develop new tissue by providing mechanical support and a temporary extracellular matrix [1–3].

The use of polymeric materials as scaffolds in tissue regeneration is well known. The polymeric scaffold plays a key role in the process of bone repair and is usually made of degradable materials that can gradually degrade with the passing of time [4–8]. For polymeric scaffolds, natural-based (e.g., chitosan, gelatin, alginate) [9–11] and synthetic-based polymers (e.g., polylactide (PLA), polycaprolactone (PCL), and polyglycolic acid (PGA)) [12–15] are the current dominant classes of materials for scaffolds in tissue engineering due to their processability, biocompatibility, possible biodegradability and similar mechanical properties to most natural tissues. Biocompatible and biodegradable natural polymers have low mechanical strength and thermal stability [16]. Synthetic polymers, on the other hand, have good mechanical properties, but their hydrophobic surfaces make fusing with the bone implant challenging [17].

PLA can be considered one of the most interesting synthetic biopolymers for tissue regeneration due to its interesting mechanical properties and good processability [18–20]. However, like other synthetic polymers, PLA is hydrophobic, thus leading to poor cell affinity by hindering cell adhesion [21]. To overcome these limits, PLA may be copolymerized or coupled with other synthetic or natural polymers [22–24].

Polycaprolactone (PCL) is a Food and Drug Administration (FDA) approved synthetic polyester that is widely used for the fabrication of tissue-engineered scaffolds [25,26]. Its advantages include a relatively slow degradation rate and lower acidic by-products compared to other polyesters.

In order to overcome the disadvantages of these biodegradable polymers, various methods, including chemical modification [27–29] and physical blend [30–33], have been designed for various biomedical applications. Chemical modifications are employed to produce new approaches for introducing various kinds of functional groups in PLA, PGA, PCL and their copolymers. For example, a novel maleated poly(lactic-co-glycolic acid) (MPLGA) material was modified by introducing reactive groups of ethanediamine or 1,4-butanediamine through direct melt ring-opening polymerization to improve its hydrophilicity and reduce the acidity in hydrolysis. In addition [34,35], copolymerization of α-hydroxy acid monomers with lysine, as an alkaline amino acid, can also be employed to introduce the alkaline functional group, amino, into the polymer side chains [36,37]. On the other hand, polymer blending is an attractive method for preparing new biomedical polymer materials because they can exhibit improvements in properties required in the biomedical field; moreover, the properties of polymer blends can be controlled by adjusting their composition ratios and blend parameters [38,39].

In the research reported here, we prepared PLL-b-PLA-b-PCL via copolymerization from morpholine-2,5-dione monomer and ε-caprolactone monomers in order to introduce alkaline amino acid, then blended PLL-b-PLA-b-PCL with PLA and prepared the porous scaffolds by using the TIPS method in order to improve the controllability of the morphologies and mechanical properties. The influences of preparation parameters, such as mass ratio, polymer concentration and freezing temperature, on the morphology, porosity and compressive strength were investigated.

2. Materials and methods

2.1. Materials

L-lysine monohydrochloride, benzyl chloroformate, N, N-dimethylformamide (DMF), 2-bromopropionyl bromide, 1,4-dioxane, L-lactide, ε-caprolactone, stannous octanoate, anhydrous ethanol and ethyl acetate were supplied by Aladdin Reagent Co., Ltd. (P. R. China). Copper sulfate, chloroform, $NaHCO_3$, $Na_2S{\cdot}9H_2O$, NaOH, and HCl were provided by China National Pharmaceutical Group Chemical Reagent Co., Ltd. (P. R. China).

2.2. Preparation of PLL-b-PLA-b-PCL and PLA

(3S,6S)-6-methyl-3-[4-(benzoxycarbonylamino)butyl]-morpholine-2,5-dione monomer was prepared from L-lysine hydrochloride, benzyl chloroformate and 2-bromoacetyl bromide using copper sulfate as a protectant according to previous reports [40,41]. Predetermined amounts of (3S, 6S)-6-methyl-3-[4-(benzyloxycarbonylamino)butyl]-morpholine-2,5-dione and ε-caprolactone with a mass ratio of 1:19 were added to an ampoule. 100 μL of 0.05 mol/L stannous isooctanoate/

chloroform solution was added and polymerized at 140 °C with a vacuum degree of 0.1 Pa for 24 hours. Finally, the obtained polymer (PLL-b-PLA-b-PCL), with a weight average molecular mass of 12.3 kDa, was purified by using chloroform and methanol for further use. PLA, with a weight-average molecular mass of 80 kDa, was prepared using ring-opening polymerization from L-lactide according to our previous literature [42].

2.3. Preparation of PLL-b-PLA-b-PCL/PLA porous scaffolds

Predetermined amounts of the PLL-b-PLA-b-PCL and PLA, with various mass ratios (1:3, 1:4, 1:5, 1:6, 1:7 and 1:8), were dissolved in 1,4-dioxane in various concentrations (14.0 wt%, 15.0 wt%, 16.0 wt%, 17.0 wt%, 18.0 wt% and 19.0 wt%). After being completely dissolved, the solutions were poured into polystyrene Petri dishes and aged in air for 6 h. The Petri dish was then placed in a refrigerator to freeze for 2 h at a predetermined temperature (-10 ℃, -20 ℃, -30 ℃ and -40 ℃), then immediately placed in a freeze dryer to remove the solvent, and the PLL-b-PLA-b-PCL/PLA scaffolds were obtained.

2.4. FTIR characterization

FTIR spectra of (3S,6S)-6-methyl-3-[4-(benzyloxycarbonylamino)butyl]-morpholine-2,5-dione and PLL-b-PLA-b-PCL were characterized with an FTIR spectrometer (Spectrum GX, Perkin Elmer Co., Ltd., USA). For the IR analysis, 1 mg of a sample was carefully mixed with 300mg of KBr and pelletized under vacuum. Then the pellets were analyzed in transmission in the range of 500–4000 cm^{-1}.

2.5 SEM measurements

The morphology and microstructure of the PLL-b-PLA-b-PCL/PLA scaffolds were characterized using scanning electron microscopy (SEM, JSM-6380LV, JEOL Co., Japan). The cross-section surfaces of the freeze-dried composite samples were cut into small pieces at -20 ℃ and coated with a thin layer of gold, and then the morphology was observed in the SEM operated at a voltage of 15 kV.

2.6. Compressive strength test

The compressive strengths (S_c) of the PLL-b-PLA-b-PCL/PLA scaffolds were tested by a universal material testing machine (Instron 1121, Instron Ltd., UK) with a 50N load cell at a constant compressive rate of 1.0 mm/min at a temperature of 25 °C. The compressive strength of the scaffold was calculated from the following Eq. (1):

$$S_c = F_{max}/A \quad (1)$$

where F_{max} is the maximum force (N) when the scaffolds collapse, and A is the compressed cross-section area (mm2) of the freeze-dried samples.

2.7. Porosity test

The porosity (P) test was performed in distilled water at 37 °C. The PLL-b-PLA-b-PCL/PLA composite scaffolds were immersed for 24 h until they were fully saturated and then the porosity of the original samples was determined from the following Eq. (2).

$$P = (W_2-W_1)/\rho V_1 \times 100\% \quad (2)$$

where W_1 and W_2 represent the weight of the scaffolds before and after immersing in the distilled water, V_1 is the volume of the scaffold before immersing, and ρ is the density of water at 37 ℃.

3. Results and discussion

3.1. FTIR analysis of PLL-b-PLA-b-PCL

The infrared spectra of (3S,6S)-6-methyl-3-[4-(benzyloxycarbonylamino)butyl]- morpholine-2,5-dione and PLL-b-PLA-b-PCL are shown in Figure 1. In the morpholine-2,5-dione spectrum, the stretching vibration peaks of ester carbonyl and

amide carbonyl were observed at 1763.13 cm^{-1} and 1691.77 cm^{-1}, respectively. The N-H stretching vibrations of amide groups were detected at 3338.71 cm^{-1} and 3199.54 cm^{-1}. For the PLL-b-PLA-b-PCL, the ester carbonyl and amide carbonyl stretching vibrations were identified at 1727.45 cm^{-1} and 1629.58 cm^{-1}, respectively, while a broad N-H stretching vibration peak was exhibited at 3417.78 cm^{-1}. The stretching vibration peaks of methyl and methylene groups in the range of 2800–3000 cm^{-1} were shared by both spectra, which collectively indicated the existence of morpholine-2,5-dione structural units in the polymer. Additionally, the methylene out-of-plane bending vibration peak at 733.31 cm^{-1} was specifically attributed to the ε-caprolactone structural units in the polymer. Therefore, the results showed that the PLL-b-PLA-b-PCL was successfully prepared.

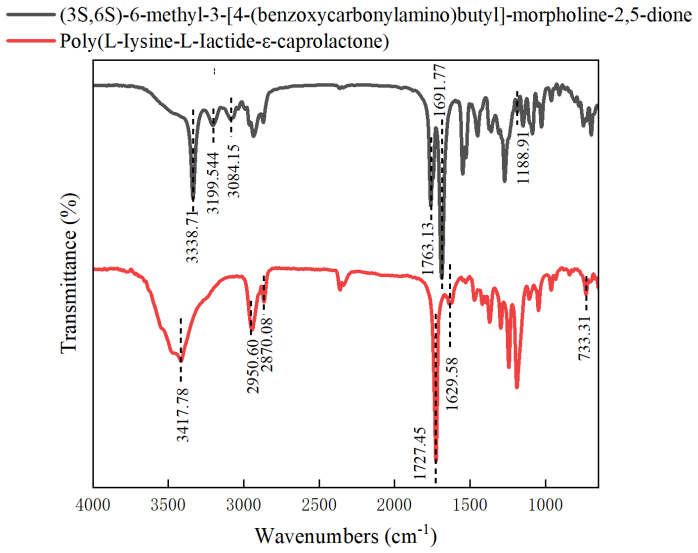

Figure 1. FTIR spectra of (3S,6S)-6-methyl-3-[4-(benzyloxycarbonylamino)butyl]- morpholine-2,5-dione and PLL-b-PLA-b-PCL.

3.2. Effect of mass ratio on the morphology of the PLL-b-PLA-b-PCL/PLA scaffolds

The effects of the mass ratio of PLL-b-PLA-b-PCL to PLA on the morphologies are shown in **Figure 2**. As the content of PLA increased, the scaffold became dense and the pore size decreased. When the mass ratio of PLL-b-PLA-b-PCL to PLA was 1:3, the scaffolds showed an irregular pore structure and the pore size was between 50 and 150 μm (**Figure 2a**). As the mass ratio of PLL-b-PLA-b-PCL to PLA was up to 1:5, the scaffolds showed a regular pore structure, and the pore size was about 30–70 μm (**Figure 2c**); this is favorable for cell growth and nutrient transportation. While the mass ratio of PLL-b-PLA-b-PCL to PLA was 1:8, the number of pores decreased, and the pore size was between 5 and 50 μm (**Figure 2f**). In these experiments, the weight average molecular mass of the PLL-b-PLA-b-PCL and PLA were 12.3 kDa and 80 kDa, respectively. When the mass ratio of PLA decreased, it meant that there were more PLL-b-PLA-b-PCL molecules with short chains in the scaffolds. The short molecule chains had higher degrees of freedom and faster movement speed than the long PLA molecule chains. In the process of TIPS for preparing the scaffolds, the fast movement of these molecular chains (PLL-b-PLA-b-PCL) could accelerate the separation of the polymer into polymer-rich phases and solvent-rich phases. During the sublimation process, the polymer-rich phase solidified and removed the solvent, forming a porous structure. The polymer scaffolds formed a relatively loose network structure, resulting in a large pore size. The cells were cultured on the surface of the scaffolds without entering into the pores when the pore size was below 20 μm; while a size above 30 μm makes it possible for the cells to penetrate into the pores [11]. Therefore, the PLL-b-PLA-b-PCL/PLA scaffolds with a ratio of 1:5 had a suitable pore size (30–70 μm) for cells to grow into them.

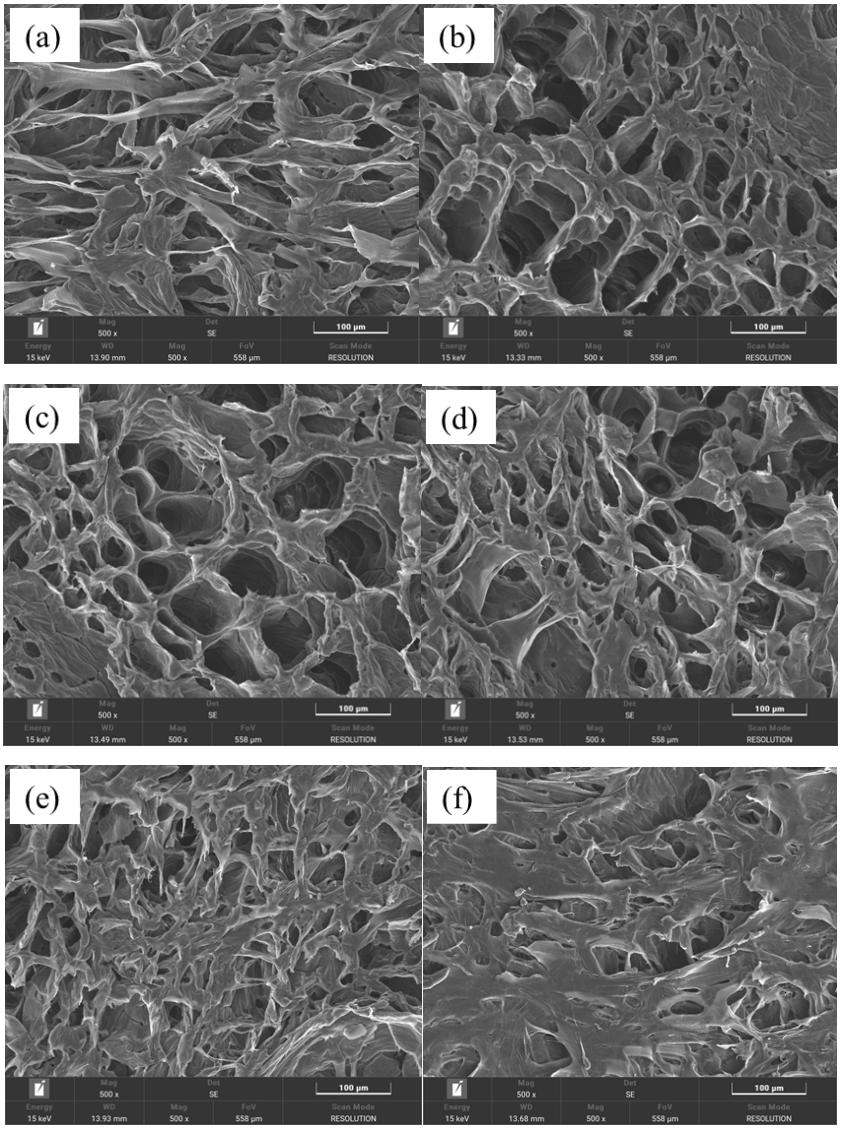

Figure 2. SEM morphology of scaffolds with mass ratios of PLL-b-PLA-b-PCL to PLA: (a) 1:3;(b) 1:4;(c) 1:5;(d) 1:6;(e) 1:7;(f)1:8, scale bars are 100 μm.

3.3. Effect of mass ratio on the porosity and compressive strength of the PLL-b-PLA-b-PCL/PLA scaffolds

The influences of mass ratio on the porosity and compressive strength are shown in **Figure 3**. As the mass ratio of pure PLA increased in the scaffold, the porosity of the scaffold also decreased, and the compressive strength increased, which was consistent with the morphologies of the scaffold displayed by SEM. As the proportion of pure PLA increased, the PLA polymer chains became long and numerous, resulting in increasing intermolecular forces of PLA. The internal skeleton structure of the scaffold became tight, leading to a decrease in pore size and porosity, and an increase in compressive strength.

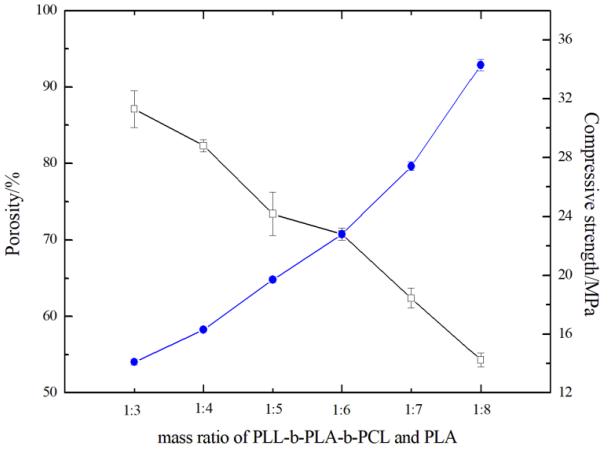

Figure 3. Effects of mass ratio on the porosity and compressive strength of the scaffolds.

3.4. Effect of PLL-b-PLA-b-PCL/PLA concentration on the morphology of the scaffolds

The morphologies of the PLL-b-PLA-b-PCL/PLA scaffolds as a function of PLL-b-PLA-b-PCL/PLA concentration are shown in **Figure 4**. When the polymer concentration was 14.0 wt% (**Figure 4a**), the pore distribution in the scaffold was uneven and irregular. When the polymer concentration reached 16.0 wt% (**Figure 4c**), the scaffold had a three-dimensional porous structure with an even pore distribution and a pore size of approximately 30–70 μm, which was helpful for nutrient transport and cell growth. As the polymer concentration exceeded 16.0 wt%, the structure became dense and the number of pores in the scaffold decreased. Therefore, the morphology and the pore size of the scaffolds could be controlled by adjusting the PLL-b-PLA-b-PCL/PLA concentration and the suitable polymer concentration was around 16.0 wt%.

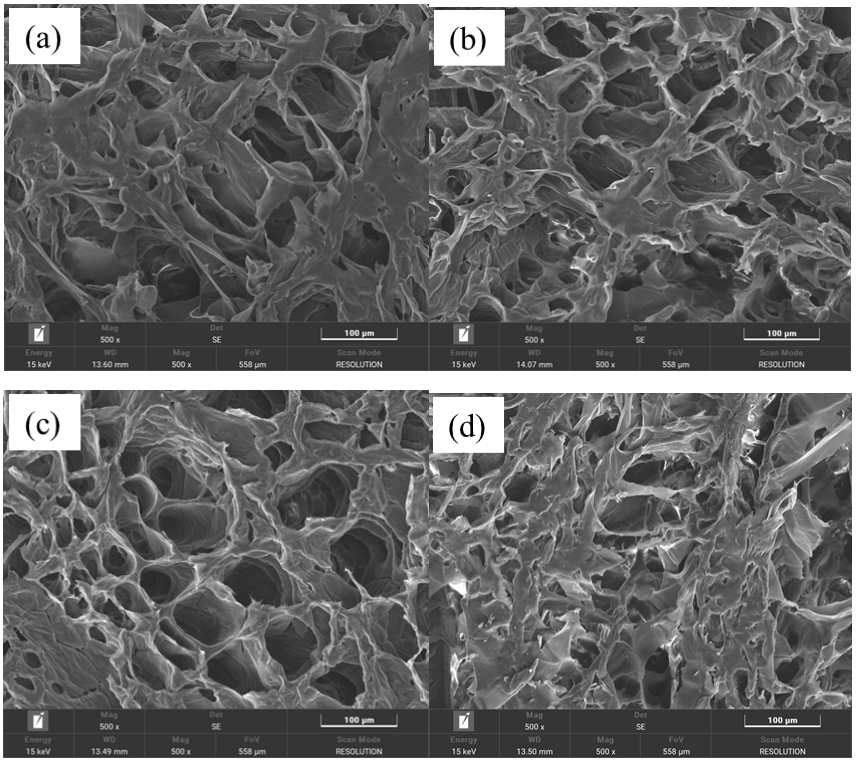

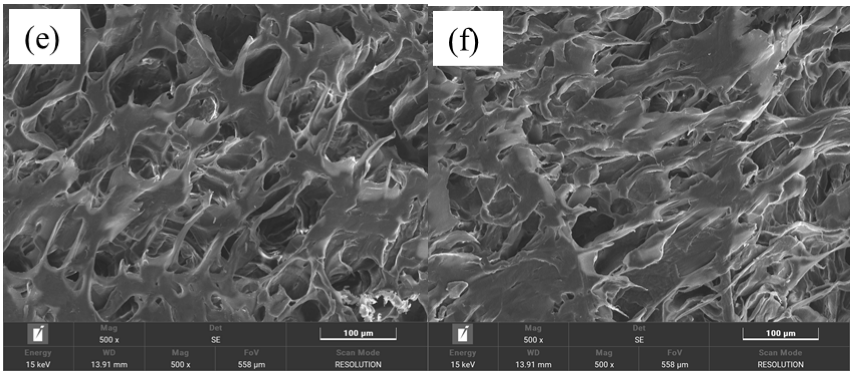

Figure 4. SEM morphology of the PLL-b-PLA-b-PCL/PLA scaffolds with various polymer concentrations: (a) 14.0 wt%; (b) 15.0 wt%; (c) 16.0 wt%; (d) 17.0 wt%; (e) 18.0 wt%; (f) 19.0 wt%, scale bars are 100 µm.

3.5. Effect of PLL-b-PLA-b-PCL/PLA concentration on the porosity and compressive strength of the scaffolds

The influences of the PLL-b-PLA-b-PCL/PLA concentration on the porosity and compressive strength of the scaffolds are shown in **Figure 5**. As the concentration of polymer increased, the porosity decreased and the compressive strength of the scaffold increased. This may be due to the fact that as the concentration of polymer increased, the free energy of the polymer solution system increased, and the interaction activity between the polymer chains in the scaffold increased. This caused the polymer chains to tend to aggregate together, resulting in a decrease in the porosity and an increase in the compressive strength of the scaffolds.

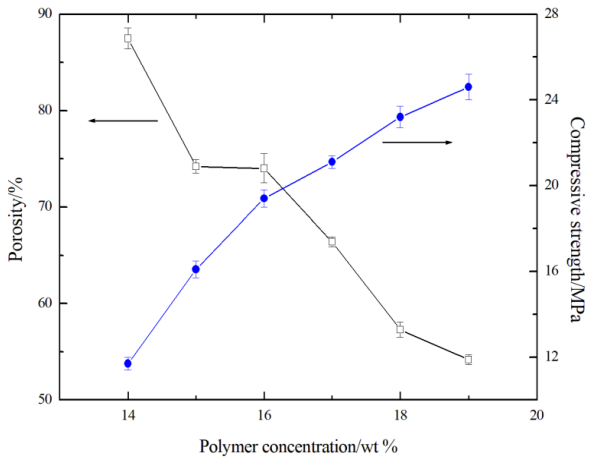

Figure 5. Effect of PLL-b-PLA-b-PCL/PLA concentration on the porosity and compressive strength of the scaffolds.

3.6. Effect of freezing temperature on the morphology of the PLL-b-PLA-b-PCL/PLA scaffolds

The morphologies of the scaffolds as a function of the freezing temperature are shown in **Figure 6**. At high freezing temperatures (-10 °C), the scaffolds showed an irregular porous structure and an uneven pore distribution. This could be explained by the fact that the thermal motion of molecules was relatively fast, and the polymer could quickly reach the separation of rich and poor phases during the process of TIPS for preparing the scaffolds, which led to an irregular pore structure. When the temperature was dropped to -30 °C, the pores became regular and the pore size was between 30 and 70 µm. This was due to the fact that the decrease in temperature slowed down the transition rate between rich and poor phases, and made the pores of the scaffold regular and evenly distributed. When the temperature was dropped to -40 °C,

the scaffolds became dense and the pore size decreased. This could be explained by the fact that the crystallization rate of 1,4-dioxane ice crystals accelerated, and the size of the formed solvent ice crystals decreased, thus the ice crystals sublimed during freeze-drying to form small pores. Therefore, it seems that -30 ℃ is acceptable for the freeze drying process and the obtained scaffolds showed a pore size of 30–70 μm.

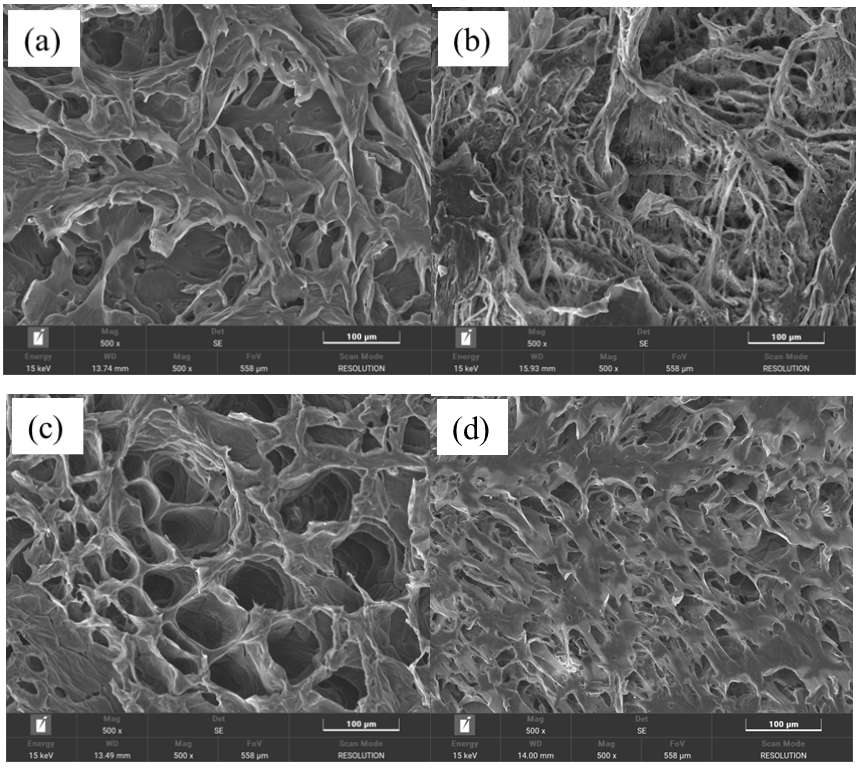

Figure 6. SEM morphology of the PLL-b-PLA-b-PCL/PLA scaffolds at various freezing temperatures: (a) -10 ℃; (b) -20 ℃; (c) -30 ℃; (d) -40 ℃, scale bars are 100 μm.

3.7. Effect of freezing temperature on the porosity and compressive strength of the PLL-b-PLA-b-PCL/PLA scaffolds

The scaffolds were prepared under controlled conditions of PLL-b-PLA-b-PCL/PLA concentration of 16.0 wt% and mass ratio of 1:5 (PLL-b-PLA-b-PCL to PLA) by varying the freezing temperatures (-10 ℃, -20 ℃, -30 ℃ and -40 ℃) and the influences of the freezing temperature on the porosity of the scaffolds are shown in **Figure 7**. As the freezing temperature decreased, the porosity of the scaffolds also decreased, while the compressive strength of the porous scaffold material increased. The effect of freezing temperature on the porosity and compressive strength of scaffolds was achieved by affecting the speed of the formation of 1,4-dioxane ice crystals. At low freezing temperatures, the crystallization rate of 1,4-dioxane ice crystals accelerated, resulting in small ice crystal sizes and an increase in the number of ice crystals. During the freeze-drying process, the ice crystals sublimed and formed small pores, leading to a decrease in the porosity and an increase in the compressive strength of the scaffold.

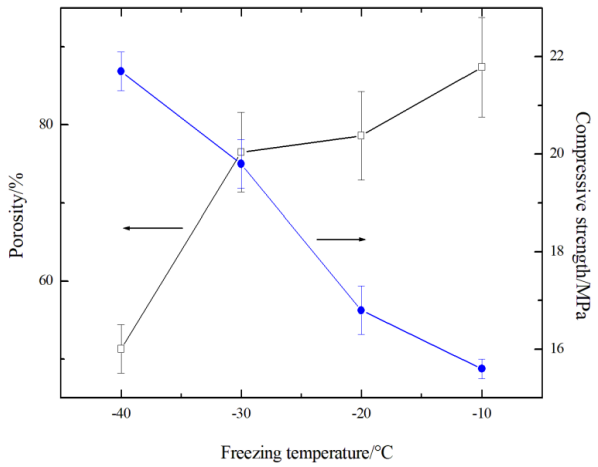

Figure 7. Effect of freezing temperature on the porosity and compressive strength of the scaffolds.

4. Conclusions

The PLL-b-PLA-b-PCL/PLA scaffolds were prepared by using the TIPS method, and the influences of the mass ratio, polymer concentration, and freezing temperature played important roles in the morphology, porosity, and compressive strength. Therefore, the structure and physical properties of the PLL-b-PLA-b-PCL/PLA scaffolds could be adjusted by changing the mass ratio, polymer concentration and freezing temperature, thus meeting the requirements of tissue and bone scaffolds.

Funding

Hunan Provincial Natural Science Foundation of China (Project No.: 2024JJ7173)

Disclosure statement

The authors declare no conflicts of interest.

References

[1] Asghari F, Samiei M, Adibkia K, et al., 2017, Biodegradable and Biocompatible Polymers for Tissue Engineering Application: A Review. Artificial Cells, Nanomedicine, and Biotechnology, 45(1): 185–192.

[2] Yousefi AM, Hoque ME, Prasad RGSV, et al., 2015, Current Strategies in Multiphasic Scaffold Design for Osteochondral Tissue Engineering: A Review. Journal of Biomedical Materials Research Part A, 103A: 2460–2481.

[3] Zhou Z, Wu W, Fang J, et al., 2021, Polymer-Based Porous Microcarriers as Cell Delivery Systems for Applications in Bone and Cartilage Tissue Engineering. International Materials Reviews, 66(2): 77–113.

[4] Ulery BD, Nair LS, Laurencin CT, 2011, Biomedical Applications of Biodegradable Polymers. Journal of Polymer Science Part B: Polymer Physics, 49(12): 832–864.

[5] Zhou ZW, Zhou ZH, Liu WJ, et al., 2020, Preparation and Degradation Behaviors of Poly(L-Lactide-Co-Glycolide-Co-ε-Caprolactone)/1,4-Butanediamine Modified Poly(Lactic-Co-Glycolic Acid) Blend Film. Journal of Macromolecular

Science Part B: Physics, 59(8): 491–501.

[6] Gastidar DD, Saha S, Chowdhury M, 2018, Porous Microspheres: Synthesis, Characterization and Applications in Pharmaceutical and Medical Fields. International Journal of Pharmaceutics, 548(1): 34–48.

[7] Wu W, Fang JJ, Liu W, et al., 2018, Preparation and Properties of BMPLGA/NBAG-β-TCP Composite Scaffold Materials. International Journal of Polymer Analysis and Characterization, 23(8): 710–720.

[8] Xie H, Qian Y, Ding J, et al., 2024, Double Enzyme Active Hydrogel Program Regulates the Microenvironment of Staphylococcus aureus-Infected Pressure Ulcers: Advanced Healthcare Materials, 2024, e2402363.

[9] Pant T, Murarka V, Jain R, et al., 2021, Chitosan-Based Microcarriers for Cellular Growth and Biologics Production. Carbohydrate Polymer Technologies and Applications, 2: 100154.

[10] Yan H, Zhou Z, Huang T, et al., 2016, Controlled Release In Vitro of Icariin from Gelatin/Hyaluronic Acid Composite Microspheres. Polymer Bulletin, 73(4): 1055–1066.

[11] Hu H, Zhou Z, Liu W, et al., 2023, Preparation of Injectable Sodium Alginate/Platelet Rich Plasma Porous Microcarriers. Journal of Macromolecular Science Part B: Physics, 62(3): 195–205.

[12] Nair LS, Laurencin CT, 2007, Biodegradable Polymers as Biomaterials. Progress in Polymer Science, 32(8–9): 762–798.

[13] Gentile P, Chiono V, Carmagnola I, et al., 2014, An Overview of Poly(Lactic-Co-Glycolic) Acid (PLGA)-Based Biomaterials for Bone Tissue Engineering. International Journal of Molecular Sciences, 15(3): 3640–3659.

[14] Liu X, Ma PX, 2004, Polymeric Scaffolds for Bone Tissue Engineering. Annals of Biomedical Engineering, 32(3): 477–486.

[15] Yang Y, Fang J, Liu W, et al., 2019, In-Vitro Degradation Behavior and Biological Properties of a Novel Maleated Poly(D,L-Lactide-Co-Glycolide) for Biomedical Applications. Journal of Macromolecular Science Part B: Physics, 58(4): 209–218.

[16] Falahati M, Ahmadvand P, Safaee S, et al., 2020, Smart Polymers and Nanocomposites for 3D and 4D Printing. Materials Today, 40: 215–245.

[17] Woodru MA, Hutmacher DW, 2010, The Return of a Forgotten Polymer-Polycaprolactone in the 21st Century. Progress in Polymer Science, 35(10): 1217–1256.

[18] Gatto ML, Furlani M, Giuliani A, et al., 2021, Biomechanical Performances of PCL/HA Micro- and Macro-Porous Lattice Scaffolds Fabricated Via Laser Powder Bed Fusion for Bone Tissue Engineering. Materials Science and Engineering C, 128: 112300.

[19] Cestari F, Petretta M, Yang Y, et al., 2021, 3D Printing of PCL/Nano-Hydroxyapatite Scaffolds Derived from Biogenic Sources for Bone Tissue Engineering. Sustainable Materials and Technologies, 29: e00318.

[20] Yang X, Wang Y, Zhou Y, et al., 2021, The Application of Polycaprolactone in Three-Dimensional Printing Scaffolds for Bone Tissue Engineering. Polymers, 13(16): 2754.

[21] Grémare A, Guduric V, Bareille R, et al., 2018, Characterization of Printed PLA Scaffolds for Bone Tissue Engineering. Journal of Biomedical Materials Research Part A, 106(3): 887–894.

[22] Hwang SW, Lee SB, Lee CK, et al., 2012, Grafting of Maleic Anhydride on Poly(L-Lactic Acid): Effects on Physical and Mechanical Properties. Polymer Testing, 31(3): 333–344.

[23] Niu XF, Luo YF, Li YG, et al., 2008, Design of Bioinspired Polymeric Materials Based on Poly(D,L-Lactic Acid) Modifications Towards Improving Its Cytocompatibility. Journal of Biomedical Materials Research Part A, 84A(4): 908–916.

[24] Jiang WR, Bao RY, Yang W, et al., 2014, Morphology, Interfacial and Mechanical Properties of Polylactide/Poly(Ethylene Terephthalate Glycol) Blends Compatibilized by Polylactide-g-Maleic Anhydride. Materials & Design, 59: 524–531.

[25] Gerçek I, Tığlı R, Gümüşderelioğlu M, 2008, A Novel Scaffold Based on Formation and Agglomeration of PCL Microbeads by Freeze-Drying. Journal of Biomedical Materials Research Part A, 86A(4): 1012–1022.

[26] Dwivedi R, Kumar S, Pandey R, Mahajan A, et al., 2020, Polycaprolactone as Biomaterial for Bone Scaffolds: Review of Literature. Journal of Oral Biology and Craniofacial Research, 10(4): 381–388.

[27] Wu W, Zhou ZH, Liu WJ, et al., 2019, Preparation and In-Vitro Degradation Behavior of Poly(L-Lactide-Co-Glycolide-Co-ε-Caprolactone) Terpolymer. Journal of Macromolecular Science Part B: Physics, 58(9): 568–577.

[28] Zhang C, Zhou Z, Liu W, et al., 2021, Preparation and Characterization of Poly(L-Lactide-Co-Glycolide-Co-ε-Caprolactone) Porous Microspheres. Journal of Macromolecular Science Part B: Physics, 60(5): 313–323.

[29] Zhang Q, Zhou Z, Peng C, et al., 2017, Preparation and Properties of Novel Maleated Poly(D,L-Lactide-Co-Glycolide) Porous Scaffolds for Tissue Engineering. Journal of Macromolecular Science Part B: Physics, 56(8): 505–515.

[30] Gu J, Zhou Z, Huang T, et al., 2022, Preparation and Properties of Poly(D,L-Lactide-Co-Glycolide-Co-ε-Caprolactone)/1,4-Butanediamine Modified Poly(Lactide-Co-Glycolide) Blend Porous Microspheres. Journal of Macromolecular Science Part B: Physics, 61(4): 270–280.

[31] Kim JY, Cho DW, 2009, Blended PCL/PLGA Scaffold Fabrication Using Multi-Head Deposition System. Microelectronic Engineering, 86(4–6): 1447–1450.

[32] de Luna MS, Filippone G, 2016, Effects of Nanoparticles on the Morphology of Immiscible Polymer Blends-Challenges and Opportunities. European Polymer Journal, 79: 198–218.

[33] Murugan S, Parcha SR, 2021, Fabrication Techniques Involved in Developing the Composite Scaffolds PCL/HA Nanoparticles for Bone Tissue Engineering Applications. Journal of Materials Science: Materials in Medicine, 32(8): 93.

[34] Cui J, Zhou Z, Yang Y, et al., 2017, Synthesis, Characterization, and Degradation Behaviors of Poly(D,L-Lactide-Co-Glycolide) Modified by Maleic Anhydride and Ethanediamine. International Journal of Polymer Analysis and Characterization, 22(7): 575–586.

[35] Zhang Q, Fang J, Liu W, et al., 2018, Synthesis and Characterization of Poly(D,L-Lactide-Co-Glycolide) Modified by Maleic Anhydride and 1,4-Butanediamine. International Journal of Polymer Analysis and Characterization, 23(5): 474–482.

[36] Annamalai DA, Hilaj E, Singh M, et al., 2024, Polylysine in Biomedical Applications: From Composites to Breakthroughs. Biomedical Materials, 19(6): 062002.

[37] Zhu H, Liu R, Shang Y, et al., 2022, Polylysine Complexes and Their Biomedical Applications. Engineering Regeneration, 4: 20–27.

[38] Peng Z, Zou T, 2019, In-Vitro Degradation Behaviors of Composite Scaffolds Based on 1,4-Butadnediamine Modified Poly(Lactide-Co-Glycolide) and Nanobioceramics. Journal of Macromolecular Science Part B: Physics, 58(8): 505–517.

[39] Wu D, Zhang Y, Zhang M, et al., 2009, Selective Localization of Multiwalled Carbon Nanotubes in Poly(Epsilon-Caprolactone)/Polylactide Blend. Biomacromolecules, 10(2): 417–424.

[40] Kidchob T, Kimura S, Imanishi Y, 1998, Degradation and Release Profile of Microcapsules Made of Poly[L-Lactic Acid-Co-L-Lysine(Z)]. Journal of Controlled Release, 54(3): 283–292.

[41] Bourkaib MC, Delaunay S, Framboisier X, et al., 2020, N-Acylation of L-Amino Acids in Aqueous Media: Evaluation of the Catalytic Performances of Streptomyces ambofaciens Aminoacylases. Enzyme and Microbial Technology, 137: 109536.

[42] Zhou Z, Liu L, Liu Q, et al., 2013, Biological Assessment of Composite Materials Based on Poly-L-Lactide and Bovine Bone. International Journal of Polymeric Materials, 62(2): 81–84.